

Pressure-induced phase transitions in AgCl, AgBr, and AgI

S. Hull* and D. A. Keen

The ISIS Facility, Rutherford Appleton Laboratory, Didcot, Oxfordshire, OX11 0QX, United Kingdom

(Received 18 August 1998)

The structural behavior of the three silver (I) halides AgCl, AgBr, and AgI has been investigated to pressures $p \sim 13$ –16 GPa using angle-dispersive x-ray diffraction with an image-plate device. Principal attention has been paid to the structural characterization of the phase transitions in the pressure range $p \sim 7$ –13 GPa observed previously by optical and resistivity techniques. In AgCl, the ambient-pressure rocksalt-structured phase transforms at $p = 6.6(6)$ GPa to a monoclinic structure with a KOH-type arrangement and then to an orthorhombic TII-type configuration at $p = 10.8(8)$ GPa. Both these structures can be considered to be more densely packed arrangements derived from rocksalt and possess ionic environments intermediate between the octahedrally coordinated rocksalt structure and an eightfold coordinated CsCl-type one adopted at higher pressure. AgBr and AgI both undergo rocksalt→KOH-type structural transitions, at $p = 7.9(4)$ GPa and $p = 11.3(2)$ GPa, respectively. The nature of the pressure-induced rocksalt→CsCl transformation in the three Ag(I) halides is discussed in relation to the continuous rhombohedral deformation model due to Buerger and to recent theoretical predictions derived from *ab initio* electronic structure calculations. [S0163-1829(99)02702-2]

I. INTRODUCTION

The structural behavior of binary AB compounds under hydrostatic pressure has been a popular topic in condensed-matter research over the past decade. The improvements in high-pressure diffraction techniques using both neutron¹ and x-ray² radiations give data suitable for Rietveld refinement and the resultant information concerning the relative stability of various structures provides a challenge to theoretical attempts to derive reliable interatomic potentials for these systems.^{3–12} The most covalent AB compounds are the III-V and II-VI semiconductors which, at ambient conditions, generally adopt the tetrahedrally coordinated zincblende or wurtzite structure. By analogy with the behavior of elemental Si and Ge under compression, many of these phases were originally thought to adopt a diatomic version of the tetragonal β -Sn structure at high pressure [i.e., InSb (Ref. 13) and GaP (Ref. 14)]. In other cases, the first transition is to the octahedrally coordinated rocksalt arrangement, followed by the β -Sn structure at higher pressures [i.e., InP (Ref. 15) and CdTe (Ref. 16)]. However, recent x-ray diffraction studies have found no evidence for ordered β -Sn-type phases in any III-V or II-VI systems and the correct description of the high-pressure phase is orthorhombic (space group $Cmcm$), in which both atomic species adopt distorted fivefold coordinations (see Refs. 17 and 18, and references therein). At the other extreme, the highly ionic Na, K, and Rb halides adopt the rocksalt structure at ambient conditions and, under pressure, the majority of these compounds undergo first-order structural phase transitions from sixfold- to the eightfold-coordinated CsCl structure.¹⁹ The CsCl structure is, in turn, adopted by the Cs halides at ambient conditions and represents the densest packing of spheres of different size. As a result, further structural transitions require extremely large pressures and, in the case of CsI, the material becomes metallic at $p > 100$ GPa and the essentially identical ionic cores adopt a dense packing which is close to hexagonal close packed (for further details, see Refs. 20 and 21).

In contrast to the general picture given above, the high-pressure structural behavior of compounds whose bonding character is intermediate between ionic and covalent is often rather complex. This is the case for the Ag(I) and Cu(I) halides, which can be considered as I-VII compounds lying at the ionic end of the sequence IV→III-V→II-VI→I-VII. Starting with the purely covalent elements Si and Ge, the degree of ionic character increases with increasing separation of the constituent elements within the periodic table through the III-V and II-VI semiconductors. On the Phillips scale of ionicity,²² the Ag and Cu monohalides have values from $f = 0.692$ (CuI) to $f = 0.894$ (AgF) which span the critical value $f_c = 0.785$ marking the idealized boundary between predominantly “covalent” and “ionic” systems. This is illustrated by the fact that AgF, AgCl, and AgBr adopt the octahedrally coordinated rocksalt structure characteristic of ionic bonding at ambient pressure and temperature, while the three Cu halides possess the zincblende arrangement favored by the more covalent compounds.²³ AgI differs only slightly from the latter, usually existing as a two-phase mixture of the cubic zincblende polymorph and its hexagonal wurtzite counterpart.²⁴

The Ag (Cu) atom possesses a completely filled $4d^{10}$ ($3d^{10}$) shell and a single $5s$ ($4s$) electron which is transferred to the halide atom. However, the Ag (Cu) halides differ from their alkali halide counterparts because the $4d$ ($3d$) electrons undergo hybridization with the halide p state. There have been several attempts to develop *ab initio* theoretical models to describe this resultant, more complex, electronic band structure, within the local-density approximation using a pseudopotential plane-wave method.^{9–12} These studies have been motivated by the extensive use of mixed phase AgBr-AgI in photographic applications.²⁵ The promotion of an electron from the valence band to the conduction band within the silver halide grain is an important, though relatively poorly understood, aspect of the formation of a latent image. Of greater relevance to this work, reliable calculations of the total energies and cohesive energies of the Cu(I)

and Ag(I) halides as a function of volume, using trial crystal structures, can predict the behavior of these compounds at elevated pressures.^{7,12}

This paper reports the results of a series of high-pressure x-ray diffraction studies of AgCl, AgBr, and AgI at pressures up to $p \sim 13$ –16 GPa. The crystallographic information obtained is used to resolve some of the uncertainties present in the literature concerning the high-pressure structural properties of these compounds (see next section) and to assess the ability of electronic structure calculations to predict this behavior.

II. SUMMARY OF PREVIOUS LITERATURE

While the high-pressure behavior of the Cu(I) halides has recently been extensively studied,^{26–29} the behavior of their Ag(I) counterparts is relatively poorly understood. The exception is AgF, which transforms to the CsCl arrangement at $p = 2.70(2)$ GPa (Ref. 30). Interestingly, the reverse CsCl→rocksalt transformation on decreasing pressure occurs via an intermediate phase which possesses an anti-NiAs configuration.³¹ The static compressibility studies of Bridgman³² observed pressure-induced phase transitions within both AgCl and AgBr at pressures in the region $p = 8.4$ –8.8 GPa, with volume discontinuities $\Delta V/V \sim 1.6\%$ and 1.1%, respectively. Subsequent optical^{33,34} and resistivity³⁵ measurements under pressure confirmed the presence of these transitions and observed one in AgI at $p \sim 10$ –12 GPa. However, the initial assumption that the high-pressure phases adopted the cubic CsCl structure³² was shown to be incorrect by the x-ray diffraction experiments on these systems. In the case of AgCl, Jamieson and Lawson³⁶ indexed five diffraction lines collected at $p \sim 11$ GPa in terms of a tetragonal unit cell with $a = 9.03$ Å and $c = 3.92$ Å, while Schock and Jamieson³⁷ subsequently interpreted 11 lines collected at $p \sim 9.2$ GPa with a hexagonal unit cell of $a = 4.06$ Å and $c = 7.02$ Å. For the latter, the observed peaks were shown to be consistent with $P3_121$ symmetry, suggesting a cinnabar-type (HgS) structure. This arrangement of the ions is related to rocksalt, with the formation of shorter Ag⁺-Cl⁻ distances (~ 2.0 Å) interpreted as evidence of increasing covalent character.³⁷ However, this structural assignment was later questioned by Kabalkina *et al.*,³⁸ on the grounds that the derived volume discontinuity at the transition ($\Delta V/V \sim 7.8\%$) is significantly greater than that observed by Bridgman.³² Their 17 diffraction lines collected at $p \sim 10$ GPa were indexed in terms of an orthorhombic unit cell with $a = 6.068$ Å, $b = 5.518$ Å, and $c = 3.519$ Å, and a distorted rocksalt-like arrangement (orthorhombic HgO type³⁸). However, the calculated intensities for such a structure were in relatively poor agreement with those observed. In the most recent work, Kusaba *et al.*³⁹ used energy-dispersive x-ray diffraction methods to determine the presence of three transitions in AgCl at $p \sim 8$ GPa, $p \sim 13$ GPa, and $p \sim 17$ GPa, though the latter required heating to $T \sim 500$ K. Diffraction patterns collected within the stability fields of the three high-pressure polymorphs were indexed as monoclinic [$a = 3.517(2)$ Å, $b = 3.988(2)$ Å, $c = 5.225(2)$ Å, $\beta = 101.00(5)^\circ$ at $p \sim 9$ GPa], orthorhombic [$a = 3.350(2)$ Å, $b = 9.916(7)$ Å, $c = 4.093(1)$ Å at $p \sim 13.5$ GPa], and cubic [$a = 3.199(1)$ Å at $p \sim 17$ GPa and

$T = 520$ K]. On the basis of the observed reflection conditions, the structures and space groups were identified as KOH-type ($P2_1$), III-type ($Cmcm$), and CsCl-type ($Pm\bar{3}m$), respectively, though no comparison of the observed intensities with those expected was reported to confirm these structural assignments. The single x-ray diffraction study of AgBr reported only three measured diffraction lines³⁷ which, by analogy with the situation in AgCl at that time, were interpreted as evidence of a cinnabar-structured phase with $a = 4.0$ Å and $c = 7.15$ Å. In the case of rocksalt-structured AgI, the transition at $p \sim 10$ –12 GPa was postulated to be to a different structure than in AgCl and AgBr, because it is accompanied by a significant blueshift in the optical absorption rather than red.³³ However, Bassett and Takahashi³⁴ and Schock and Jamieson³⁷ were unable to determine the structure of the high-pressure polymorph in AgI, merely remarking that it was not CsCl-type and providing a possible tetragonal unit cell with $a = 5.611$ Å and $c = 5.020$ Å (Ref. 37).

Very recently, Nunes *et al.*¹² have published an extensive *ab initio* study of the high-pressure structural properties of AgCl, AgBr, and AgI, using the local-density approximation with a pseudopotential plane-wave method in a number of trial structures (zincblende, wurtzite, rocksalt, β -Sn, cinnabar, NiAs, and CsCl). In their calculations of AgCl and AgBr, pressure favors a continuous transformation from the rocksalt structure to the CsCl one over the pressure ranges $p = 5$ –18 GPa and $p = 7.5$ –32 GPa, respectively. The intermediate structure is discussed as an idealized version of the trigonal cinnabar configuration in space group $P3_121$. In contrast, AgI was proposed to transform from rocksalt→CsCl in a discontinuous manner, though the structure of the intermediate phase was not determined.

III. EXPERIMENT

Commercially available AgCl, AgBr, and AgI supplied by the Aldrich Chemical Company, of stated purity 99.999%, was used in this work. Finely ground material was loaded into diamond anvil cells of the Merrill-Bassett⁴⁰ design, which allow diffraction data to be collected up to a maximum scattering angle $2\theta \sim 40^\circ$ and a maximum pressure $p \sim 15$ –17 GPa. A 4:1 mixture of methanol:ethanol was included as a pressure transmitting medium and the pressure determined using the ruby-fluorescence method. The experiments were performed on station 9.1 at the Synchrotron Radiation Source, Daresbury Laboratory, U.K. using an image plate setup² with an incident wavelength $\lambda = 0.4868(1)$ Å. Two-dimensional powder-diffraction data collected on the image plates were read on a Molecular Dynamics 400A PhosphorImager and then integrated using the PLATYPUS program⁴¹ to provide one-dimensional diffraction patterns. Least-squares refinements of the diffraction data were performed using the FULLPROF program.⁴² Further details of the fitting procedure are given for the individual phases in Secs. IV A–IV C.

IV. RESULTS

A. Silver chloride

On increasing pressure, the rocksalt structured phase AgCl-I is stable up to $p = 6.6(1)$ GPa, at which point addi-

tional reflections are observed at d spacings of ~ 1.79 , ~ 2.17 , ~ 2.62 , and ~ 3.12 Å. On further pressurizing to $p = 7.5(1)$ GPa, all the remaining diffraction peaks characteristic of the rocksalt phase disappeared and the sample was assumed to have completely transformed to phase AgCl-II. Diffraction data of high statistical quality were measured from this phase at a pressure $p = 8.6(1)$ GPa for ~ 8 h. The resultant pattern was considerably more complex than that measured from the rocksalt-structured AgCl-I, indicative of a significant reduction in symmetry. Trial calculations of the expected diffraction pattern were performed using plausible structures for this phase derived from previous work on AgCl and related compounds. These included the monoclinic KOH structure (cf. Ref. 39), the cinnabar structure (cf. Ref. 37), and the anti-NiAs structure (cf. AgF in Ref. 31). These simulations assumed a value of 37.5 Å³ for the unit-cell volume per formula unit (V/Z), which is estimated using the value $V/Z \sim 38$ Å³ observed in the rocksalt-structured phase AgCl-I at $p = 6.6(1)$ GPa. Approximate values of the various axial ratios, interaxial angles and ionic positions were estimated using ‘‘typical’’ values for compounds which adopt these structures under ambient conditions.²³

The measured diffraction pattern of AgCl-II showed the greatest resemblance to that calculated using the KOH arrangement and the agreement was improved further by adjustment of the unit-cell dimensions to $a = 3.55$ Å, $b = 4.00$ Å, $c = 5.25$ Å, and $\beta = 100.5^\circ$. All the observed diffraction peaks could be indexed with this unit cell by including the single reflection condition ($0k0$; $k = 2n$) imposed by the space group $P2_1/m$. This is consistent with the KOH structure and we initially place the Ag⁺ and Cl⁻ in the 2(e) Wyckoff sites at $(x, 1/4, z)$, with $x_{\text{Ag}} = 0.17$, $z_{\text{Ag}} = 0.29$, $x_{\text{Cl}} = 0.32$, and $z_{\text{Cl}} = 0.77$, these values being the positions adopted by K⁺ and OH⁻, respectively, in KOH itself.²³ However, significant differences between the observed and calculated intensities of several peaks suggested that these ‘‘trial’’ values were inappropriate and least-squares refinements of the diffraction data were performed. The final fit to the experimental data used a total of 13 adjustable parameters, comprising an overall scale factor, two peak width parameters, four unit-cell constants, two isotropic thermal vibration parameters (B_{Ag} and B_{Cl}), and the four ionic position parameters. The quality of the resultant fit is illustrated in Fig. 1. The values of the significant fitted parameters for the data collected at six pressures within the stability range of AgCl-II are given in Table I.

At a pressure of $p = 10.8(1)$ GPa, additional diffraction peaks not consistent with the KOH structure appear at, for example, $d \sim 2.05$ Å, ~ 2.52 Å, and ~ 3.17 Å. On further increase of pressure to $p = 12.6(1)$ GPa, the diffraction peaks from the KOH-structured phase disappeared and the AgCl sample had undergone a complete transition to a new phase which we label AgCl-III. Once again, calculations of the expected diffraction pattern using likely trial structures were performed, in this case using $V/Z = 34.5$ Å³ estimated from the smallest value observed in AgCl-II before the transition. The best agreement was obtained using the orthorhombic TII-type arrangement proposed by Kusaba *et al.*³⁹ with approximate values of $a = 3.35$ Å, $b = 10.05$ Å, and $c = 4.00$ Å at $p = 12.6(1)$ GPa. This structure places both the Ag⁺ and Cl⁻ in the 4(c) $0, y, 1/4$ positions of space group

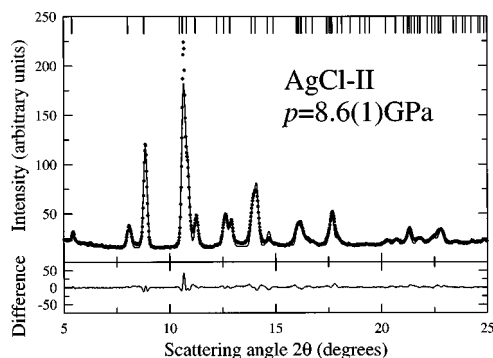


FIG. 1. Least-squares fit (solid line) to the experimental diffraction data (dots) for KOH-structured phase AgCl-II collected at $p = 8.6(1)$ GPa. The difference plot (observed minus calculated) is shown at the bottom of the figure and the calculated 2θ positions of the allowed reflections are illustrated by the tick marks across the top of the plot. The structural parameters obtained by this procedure are listed in Table I.

$Cmcm$ and the initial values $y_{\text{Ag}} = 0.39$ and $y_{\text{Cl}} = 0.13$ were taken from TI⁺ and I⁻, respectively, in TII itself.²³ Least-squares refinements of experimental data collected for ~ 6 h at $p = 14.2(1)$ GPa showed the values adopted in AgCl-III to be very close to these estimated positional parameters (see Table I). The final refinements varied the scale factor, two peak width parameters, three unit-cell constants, two isotropic thermal vibration parameters, and two positional parameters, and the agreement with the data is shown in Fig. 2.

B. Silver bromide

The rocksalt-structured phase AgBr-I was observed to undergo a structural phase transition on increasing pressure at $p = 7.9(1)$ GPa with the appearance of additional reflections at $d \sim 1.90$, ~ 2.16 , ~ 2.24 , and ~ 2.65 Å. The remaining peaks due to the rocksalt-structured phase disappeared after a further small increase in pressure to $p = 8.1(1)$ GPa. The resultant diffraction pattern of phase AgBr-II showed some similarity to that measured previously for AgCl-II, though a significant fraction of the intense reflections observed in AgCl-II (Fig. 1) were now considerably weaker. Simulations of the expected diffraction pattern from a KOH-structured phase of AgBr were performed, using the same positional parameters as AgCl-II but with the unit-cell dimensions increased with respect to those found in AgCl by an approximate factor derived from the difference in unit-cell constant for the rocksalt-structured phases. This gave a calculated diffraction pattern in good agreement with that measured, indicating that the observed intensity differences between AgCl-II and AgBr-II are purely a consequence of the different scattering powers of Cl⁻ and Br⁻ for x rays. Least-squares refinements of the data, with the same set of variables as AgCl-II, confirmed the KOH-type structure of AgBr-II and provided the fitted parameters listed in Table II. The fit to the experimental data is illustrated in Fig. 3. No further transitions were observed in AgBr up to the maximum pressure reached [$p = 12.7(1)$ GPa].

C. Silver iodide

The ambient pressure data for AgI showed that the sample was initially a mixture of the wurtzite and zincblende struc-

TABLE I. Summary of the results of the least-squares refinements of the diffraction data collected from AgCl over the pressure range $p=0-16.1(1)$ GPa. Phases I, II, and III adopt the rocksalt, KOH and TII structures, respectively.

Pressure p (GPa)	Phase	Lattice parameters			β ($^\circ$)	Thermal parameters		Positional parameters					
		a (\AA)	b (\AA)	c (\AA)		B_{Ag} (\AA^2)	B_{Cl} (\AA^2)	x_{Ag}	y_{Ag}	z_{Ag}	x_{Cl}	y_{Cl}	z_{Cl}
0.0	I	5.5463(2)	$=a$	$=a$	90	5.5(2)	3.2(3)	1/2	1/2	1/2	0	0	0
2.5	I	5.4610(3)	$=a$	$=a$	90	5.4(3)	2.9(4)	1/2	1/2	1/2	0	0	0
3.9	I	5.4138(6)	$=a$	$=a$	90	5.4(5)	2.6(7)	1/2	1/2	1/2	0	0	0
5.2	I	5.3820(3)	$=a$	$=a$	90	5.5(3)	3.3(4)	1/2	1/2	1/2	0	0	0
6.2	I	5.3537(3)	$=a$	$=a$	90	6.0(3)	3.3(4)	1/2	1/2	1/2	0	0	0
6.6	I	5.346(2)	$=a$	$=a$	90	7.1(6)	3.7(6)	1/2	1/2	1/2	0	0	0
6.6	II	3.587(5)	3.992(6)	5.307(7)	98.40(5)	7.4(7)	3.3(5)	0.184(3)	1/4	0.220(3)	0.300(4)	1/4	0.713(4)
7.6	II	3.561(3)	3.994(4)	5.271(5)	99.12(4)	6.7(5)	2.7(4)	0.177(2)	1/4	0.224(2)	0.298(3)	1/4	0.711(2)
7.9	II	3.548(3)	3.997(3)	5.259(4)	99.75(3)	5.8(5)	3.0(4)	0.165(2)	1/4	0.215(2)	0.307(5)	1/4	0.700(3)
8.6	II	3.530(2)	4.011(2)	5.243(2)	100.69(2)	5.8(3)	3.3(4)	0.157(1)	1/4	0.210(2)	0.308(3)	1/4	0.705(3)
10.0	II	3.497(2)	4.009(2)	5.214(2)	102.11(3)	4.7(3)	3.2(4)	0.148(1)	1/4	0.206(2)	0.314(3)	1/4	0.702(3)
10.8	II	3.481(5)	4.016(5)	5.191(6)	102.87(5)	4.8(5)	2.8(5)	0.138(3)	1/4	0.210(3)	0.322(4)	1/4	0.696(4)
10.8	III	3.399(3)	10.124(6)	4.032(3)	90	5.1(5)	2.2(5)	0	0.404(2)	1/4	0	0.141(2)	1/4
12.7	III	3.369(1)	10.023(3)	4.053(1)	90	3.9(2)	2.4(3)	0	0.397(1)	1/4	0	0.138(1)	1/4
14.2	III	3.337(1)	9.907(3)	4.095(1)	90	3.9(2)	2.7(3)	0	0.398(1)	1/4	0	0.140(1)	1/4
16.1	III	3.320(1)	9.835(2)	4.108(1)	90	3.8(2)	2.5(3)	0	0.398(1)	1/4	0	0.141(1)	1/4

tured phases (AgI-II and AgI-II', respectively). As illustrated in Fig. 4, the p - T phase diagram of AgI in the low-pressure region ($p < \sim 1$ GPa) is rather complex.^{43,44} The structural behavior of the material in this region has been extensively studied, including the determination of the tetragonal structure of phase AgI-IV (Ref. 45), which is intermediate between the tetrahedrally and octahedrally coordinated structures, the effects of pressure on the superionic behavior in the body-centred-cubic structured phase AgI-I (α -AgI),⁴⁴ and the onset of thermally induced disorder within AgI-III as the rocksalt-structured phase is heated.^{44,46,47} As a consequence, measurements in this work began at $p=1.5(1)$ GPa. The rocksalt-structured phase AgI-III was found to be stable up to $p=11.1(1)$ GPa. A further small increase in pressure to $p=11.3(1)$ GPa produced an abrupt change in the diffraction pattern, with peaks at d spacings of ~ 2.12 , ~ 2.65 , ~ 2.78 , and ~ 2.86 \AA and no evidence of any remaining AgI-

III. The diffraction pattern from the high-pressure phase, which we label AgI-V, was very similar to that measured from AgBr-II. This clearly implies that the structure of AgI-V is the same KOH-type as AgCl-II and AgBr-II, despite the suggestions of Slykhouse and Drickamer³³ that the differing behavior of the optical properties at the transitions imply they are not. The same procedure as described in Sec. IV B was followed, with simulations of the diffraction performed with approximate starting values for the unit-cell constants and subsequent refinements of the diffraction data to obtain fitted values of the unit-cell constants, ionic position parameters, etc. However, the quality of the fit to the data for AgI-V was somewhat poorer than that obtained for the isostructural AgCl-II and AgBr-II phases. Closer inspection showed that the intensities of the peaks with predominantly $00l$ character were systematically underestimated in the calculated pattern, indicating a degree of preferred orien-

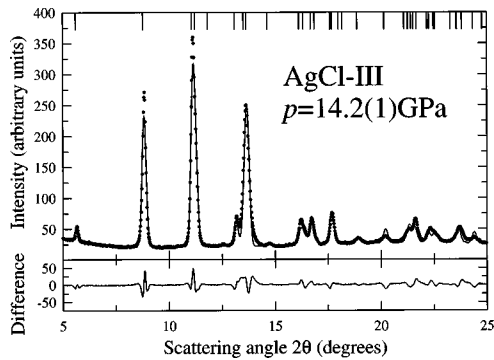


FIG. 2. Least-squares fit (solid line) to the experimental diffraction data (dots) for TII-structured phase AgCl-III collected at $p=14.2(1)$ GPa. The difference plot (observed minus calculated) is shown at the bottom of the figure and the calculated 2θ positions of the allowed reflections are illustrated by the tick marks across the top of the plot. The structural parameters obtained by this procedure are listed in Table I.

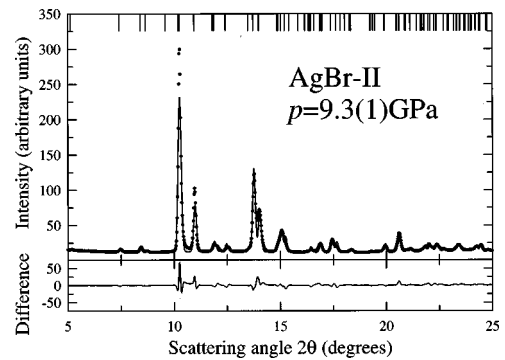


FIG. 3. Least-squares fit (solid line) to the experimental diffraction data (dots) for KOH-structured phase AgBr-II collected at $p=9.3(1)$ GPa. The difference plot (observed minus calculated) is shown at the bottom of the figure and the calculated 2θ positions of the allowed reflections are illustrated by the tick marks across the top of the plot. The structural parameters obtained by this procedure are listed in Table II.

TABLE II. Summary of the results of the least-squares refinements of the diffraction data collected from AgBr over the pressure range $p=0-12.7(1)$ GPa. Phases I and II adopt the rocksalt and KOH structures, respectively.

Pressure p (GPa)	Phase	Lattice parameters				Thermal parameters		Positional parameters					
		a (Å)	b (Å)	c (Å)	β (°)	B_{Ag} (Å ²)	B_{Br} (Å ²)	x_{Ag}	y_{Ag}	z_{Ag}	x_{Br}	y_{Br}	z_{Br}
0.0	I	5.7721(2)	= a	= a	90	6.3(4)	3.3(3)	1/2	1/2	1/2	0	0	0
1.5	I	5.7103(2)	= a	= a	90	6.5(4)	3.3(2)	1/2	1/2	1/2	0	0	0
3.9	I	5.6344(2)	= a	= a	90	6.5(4)	3.2(3)	1/2	1/2	1/2	0	0	0
6.2	I	5.5673(3)	= a	= a	90	6.0(4)	2.8(3)	1/2	1/2	1/2	0	0	0
7.9	I	5.5203(4)	= a	= a	90	7.9(7)	3.7(4)	1/2	1/2	1/2	0	0	0
7.9	II	3.821(7)	3.980(7)	5.513(9)	95.9(1)	5.5(6)	3.3(4)	0.18(1)	1/4	0.21(1)	0.28(1)	1/4	0.69(1)
8.1	II	3.818(4)	3.981(3)	5.510(6)	96.07(8)	4.9(7)	2.7(6)	0.182(6)	1/4	0.215(4)	0.284(6)	1/4	0.686(5)
9.0	II	3.791(2)	3.984(2)	5.496(2)	97.05(5)	4.5(5)	2.9(4)	0.161(3)	1/4	0.216(3)	0.291(3)	1/4	0.689(3)
9.3	II	3.787(2)	3.985(2)	5.487(3)	97.94(3)	5.5(7)	2.3(4)	0.152(3)	1/4	0.227(3)	0.298(3)	1/4	0.706(3)
10.2	II	3.749(2)	4.007(2)	5.464(3)	98.56(4)	5.7(5)	2.7(4)	0.133(3)	1/4	0.223(3)	0.302(3)	1/4	0.696(3)
12.7	II	3.691(2)	4.018(2)	5.450(2)	100.87(4)	6.5(4)	3.2(3)	0.129(2)	1/4	0.229(2)	0.305(3)	1/4	0.680(3)

tation within the sample. As a result, an additional variable was included in the fit to represent the 00 l preferred orientation of grains, following the model of March.⁴⁸ This produced a marked improvement in the quality of the fit (see Fig. 5) and provided the fitted parameters listed in Table III.

D. General trends

The presence of the structural phase transitions at pressures of $p=6.6(6)$ GPa and $p=10.8(8)$ GPa in AgCl and at $p=7.9(4)$ GPa and $p=11.3(2)$ GPa in AgBr and AgI, respectively, are broadly in agreement with the results of previous studies using x-ray diffraction, optical and resistivity techniques.³²⁻³⁹ The compressibility data for the three Ag(I) halides shown in Figs. 6-8 can be used to determine the isothermal bulk moduli (B_0) of the various polymorphs by fitting the Birch equation⁴⁹

$$p = \frac{3}{2} B_0 \left[\left[\frac{V_0}{V(p)} \right]^{7/3} - \left[\frac{V_0}{V(p)} \right]^{5/3} \right] \times \left[1 - \frac{3}{4} (4 - B_0') \left[\left[\frac{V_0}{V(p)} \right]^{2/3} - 1 \right] \right]$$

to the experimental data for $V(p) = V_u/Z$, where V_u is the unit-cell volume determined from the experimental values of the unit-cell constants, Z is the number of formula units in the unit cell, and V_0 is the value of $V(p)$ at ambient pressure.

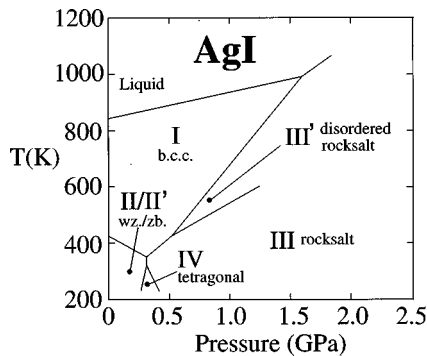


FIG. 4. The complex p - T phase diagram of AgI in the low-pressure region (after Refs. 43, 44).

In practice, attempts to vary the first pressure derivative of the bulk modulus (B_0') away from its nominal value of 4.0 did not yield significant improvements in the quality of the fit. This is a consequence of the limited pressure range over which a given phase is stable. The values of B_0 were, therefore, determined with the fixed value $B_0'=4$. Values of $B_0 = 47(1)$ GPa, $B_0 = 45(1)$ GPa, and $B_0 = 43(1)$ GPa are determined for the rocksalt-structured phases of AgCl, AgBr, and AgI, respectively. These are slightly higher than those obtained in previous studies using, for example, ultrasonic pulse techniques ($B_0 = 44-46$ GPa for AgCl and $B_0 = 40-42$ GPa for AgBr [Refs. 50-52]) but somewhat lower than those calculated by *ab initio* methods ($B_0 = 66.8$ GPa and $B_0 = 60.3$ GPa for AgCl and AgBr, respectively¹²). The latter is probably a consequence of the neglect of thermal effects in the calculations and the agreement would be expected to be better in comparison with low-temperature experimental data for B_0 . Interestingly, the expected trend of increasing compressibility in the sequence AgCl \rightarrow AgBr \rightarrow AgI observed for the rocksalt phases is reversed for the KOH structured polymorphs, with values of $B_0 = 63(3)$ GPa, $B_0 = 75(4)$ GPa, and $B_0 = 89(6)$ GPa, re-

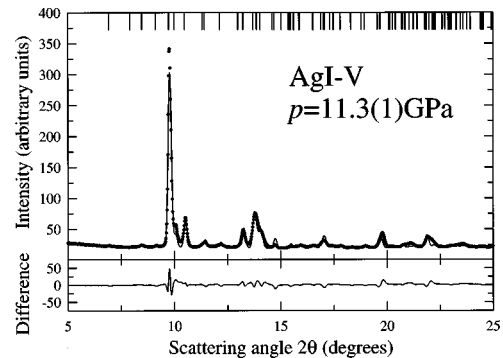


FIG. 5. Least-squares fit (solid line) to the experimental diffraction data (dots) for KOH-structured phase AgI-V collected at $p = 11.3(1)$ GPa. The difference plot (observed minus calculated) is shown at the bottom of the figure and the calculated 2θ positions of the allowed reflections are illustrated by the tick marks across the top of the plot. The structural parameters obtained by this procedure are listed in Table III.

TABLE III. Summary of the results of the least-squares refinements of the diffraction data collected from AgI over the pressure range $p=0-14.5(1)$ GPa. Phases II, II', III, and V adopt the wurtzite, zincblende, rocksalt, and KOH structures, respectively.

Pressure p (GPa)	Phase	Lattice parameters				Thermal parameters		Positional parameters					
		a (Å)	b (Å)	c (Å)	β (°)	B_{Ag} (Å ²)	B_{I} (Å ²)	x_{Ag}	y_{Ag}	z_{Ag}	x_{I}	y_{I}	z_{I}
0.0	II'	6.4991(7)	$=a$	$=a$	90	6.5(5)	5.6(4)	1/4	1/4	1/4	0	0	0
0.0	II	4.599(3)	$=a$	7.524(5)	$\gamma=120$	8.9(7)	5.8(7)	0	0	0	0	0	0.335(6)
1.5	III	6.0339(2)	$=a$	$=a$	90	8.1(6)	5.3(4)	1/2	1/2	1/2	0	0	0
3.4	III	5.9577(3)	$=a$	$=a$	90	7.1(7)	5.5(4)	1/2	1/2	1/2	0	0	0
6.4	III	5.8570(3)	$=a$	$=a$	90	7.0(6)	5.3(4)	1/2	1/2	1/2	0	0	0
8.9	III	5.7894(3)	$=a$	$=a$	90	6.7(7)	4.4(3)	1/2	1/2	1/2	0	0	0
11.1	III	5.7320(4)	$=a$	$=a$	90	6.4(8)	5.0(3)	1/2	1/2	1/2	0	0	0
11.3	V	4.056(1)	4.057(2)	5.615(3)	98.43(4)	4.2(2)	3.4(2)	0.157(4)	1/4	0.219(4)	0.300(3)	1/4	0.707(3)
11.7	V	4.052(1)	4.052(1)	5.604(3)	98.70(4)	3.9(2)	2.9(3)	0.157(4)	1/4	0.217(3)	0.300(3)	1/4	0.704(3)
14.3	V	4.007(2)	4.064(2)	5.546(6)	100.39(8)	3.5(3)	2.9(3)	0.150(5)	1/4	0.228(4)	0.307(4)	1/4	0.697(3)
14.5	V	4.001(1)	4.067(1)	5.545(5)	100.55(8)	3.5(3)	2.7(3)	0.150(5)	1/4	0.230(4)	0.308(4)	1/4	0.695(3)

spectively. The relatively large uncertainties in these values are a consequence of the limited pressure range over which data are measured. The values for the volume discontinuities at the rocksalt→KOH transitions are $\Delta V/V_0=1.60(5)\%$, $0.96(7)\%$, and $3.2(2)\%$ for AgCl, AgBr, and AgI, respectively. The first two agree well with the values of 1.6% and 1.1% originally determined by Bridgman³² using static compressibility techniques. The KOH→III transition in AgCl is accompanied by a volume change $\Delta V/V_0\sim 1.9(2)\%$.

V. DISCUSSION

As discussed in Sec. I, binary compounds with the rocksalt structure generally transform to the CsCl arrangement at elevated pressure, provided the bonding is predominantly ionic in character. In the I-VII compounds, such behavior has been observed in AgF at $p\sim 2.70(2)$ GPa (Ref. 30), in AgCl

at $p\sim 17$ GPa and $T\sim 500$ K (Ref. 39) and presumably occurs in AgBr and AgI at somewhat higher pressures. In considering the nature of the pressure-induced rocksalt→CsCl structural transformation there are several possibilities.

(i) The transition is first-order reconstructive with an abrupt volume decrease. Simple “hard-sphere” calculations for a binary AB compound show that the ratio of the volumes of the CsCl and rocksalt (RS) arrangements is dependent on the ratio of the radii r_A/r_B as follows:

$$V_{\text{CsCl}}/V_{\text{RS}}=4\sqrt{3}/9=0.770, \quad \text{if } r_A/r_B>\sqrt{3}-1=0.732,$$

$$V_{\text{CsCl}}/V_{\text{RS}}=\frac{4}{(1+r_A/r_B)^3}, \quad \text{if } 0.732\geq r_A/r_B\geq 0.414$$

and

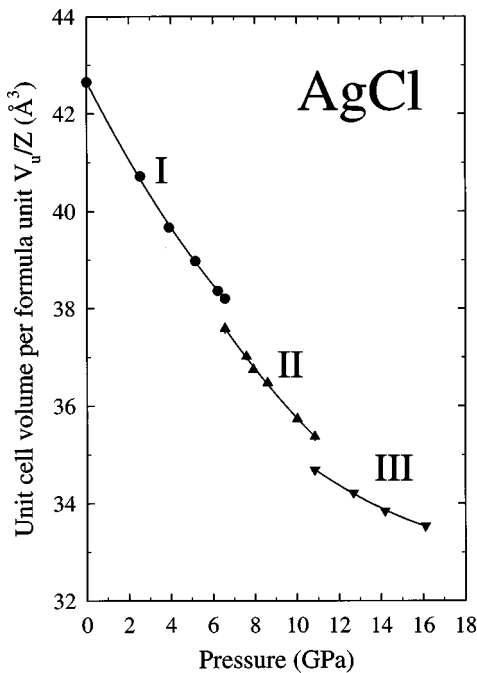


FIG. 6. The compressibility of AgCl under pressure illustrated by the decrease in the unit-cell volume per formula unit (V_u/Z).

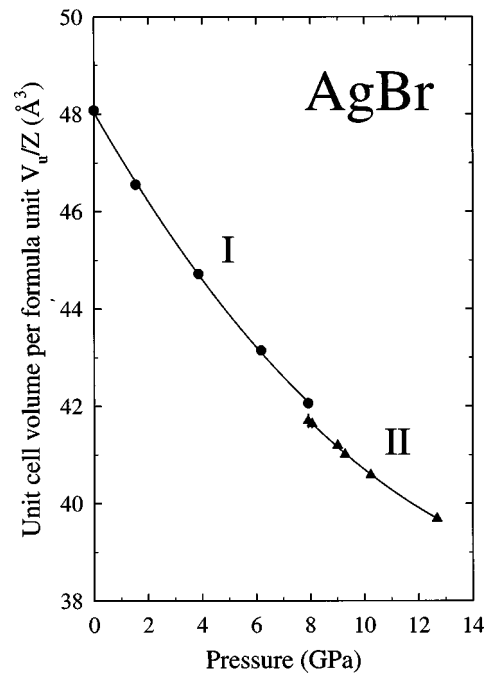


FIG. 7. The compressibility of AgBr under pressure illustrated by the decrease in the unit-cell volume per formula unit (V_u/Z).

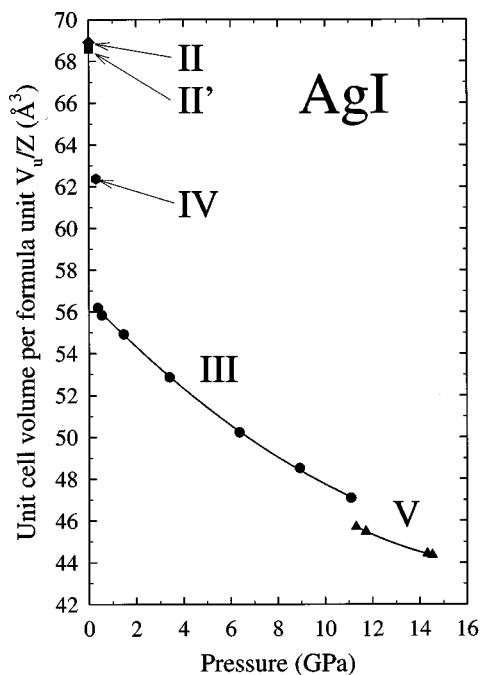


FIG. 8. The compressibility of AgI under pressure illustrated by the decrease in the unit-cell volume per formula unit (V_u/Z). The data for the tetragonal phase AgI-IV and the two lowest pressure points in the rocksalt-structured phase AgI-III are taken from Ref. 45.

$$V_{\text{CsCl}}/V_{\text{RS}} = \sqrt{2} = 1.414, \quad \text{if } r_A/r_B < \sqrt{2} - 1 = 0.414.$$

So, provided the anion and cation are of comparable size, the idealized rocksalt→CsCl transition is accompanied by a $\sim 23\%$ volume decrease. In practice, the volume discontinuity is somewhat smaller than this value, typically in the range 10–15 % (see Refs. 53, 54, and references therein).

(ii) The transition occurs via more than one first-order structural transition, involving intermediate phases of lower symmetry and more, but smaller, discontinuities during the reduction in $V(p)$ with pressure p . This behavior has been reported in PbS, PbSe, and PbTe, where the rocksalt→CsCl transition occurs via intermediate phases with the orthorhombic GeS or TlI structures.⁵⁵ The high-pressure behavior of AgF can be considered intermediate between those described in (i) and (ii), undergoing a direct transformation from rocksalt to CsCl on increasing pressure [$V_{\text{CsCl}}/V_{\text{RS}} = 0.884(4)$] but the reverse transition on decreasing pressure occurs via an intermediate phase with the anti-NiAs structure.³¹

(iii) The transition is continuous, evolving via a gradual distortion of the cubic unit cell. There are a number of topological possibilities for the displacive rocksalt→CsCl transformation (see Ref. 56, and references therein), the most straightforward being proposed by Buerger⁵⁷ and considers the primitive rhombohedral unit cell as illustrated in Fig. 9. In this scheme, the rhombohedral angle α increases continuously from 60° (rocksalt) to 90° (CsCl), such that the $[110]$ cubic direction in the former becomes the $[110]$ direction in the latter.

The presence of KOH and TlI structured phases between the rocksalt and CsCl-structured modifications and the small volume discontinuities at the transitions clearly indicate that AgCl (and presumably AgBr and AgI) follow route (ii).

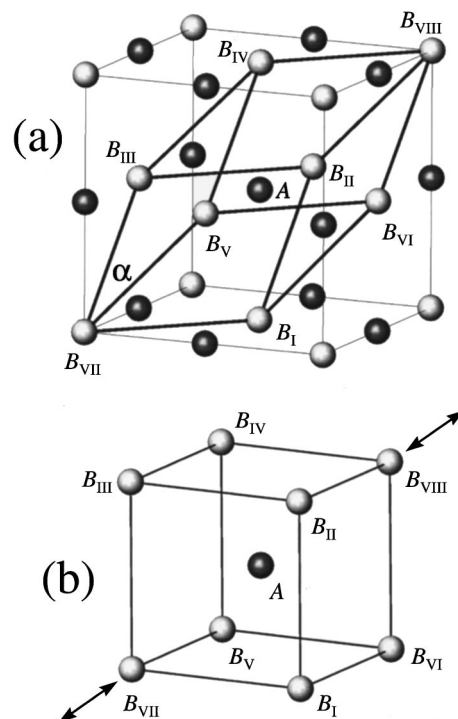


FIG. 9. Schematic representation of the continuous rhombohedral deformation of the rocksalt structure (a), to the CsCl arrangement (b), in a binary AB compound proposed by Buerger (Ref. 57). The transformation from sixfold to eightfold coordination is associated with an increase in the rhombohedral angle α from 60° to 90° .

However, we will start by discussing the continuous transformation model (iii) in more detail, in order to relate the experimental evidence to recent theoretical¹² and x-ray diffraction³⁹ studies which have been interpreted in terms of a displacive mechanism, and to provide a clearer description of the sequence of structural changes in these compounds. In their idealized forms, the two displacive mechanisms^{12,39} are topologically equivalent to each other and to the Buerger model⁵⁷ illustrated in Fig. 9. The development of these two differing descriptions, summarized in Table IV, are motivated by the desire to interpret the conflicting experimental evidence. Nunes *et al.*¹² did not consider the experimental results of Kusaba *et al.*³⁹ and instead related their calculations to the earlier proposed structures.³⁷

Model 1. The *ab initio* electronic structure calculations of Nunes *et al.*¹² indicated that the likely transitional route between rocksalt and CsCl structures in AgCl and AgBr was via a trigonal phase in space group $P3_121$. This structure places the two ionic species in $3(a)$ and $3(b)$ Wyckoff sites, i.e., in positions at $x_A, 0, 1/3$, etc. and $x_B, 0, 5/6$, etc. with $x_A = x_B = 2/3$. This arrangement can be considered as an idealized variant of the cinnabar structure, of the type proposed for the high-pressure phase of AgCl and AgBr on the basis of an early x-ray diffraction study.³⁷ The rocksalt→CsCl transformation then involves no changes in the ionic coordinates, merely a decrease in the trigonal unit cell axial ratio such that c/a reduces from $\sqrt{6}$ to $\sqrt{3}/2$. In many cinnabar-structured compounds, the values of the positional parameters are generally rather displaced from the $x_A = x_B = 2/3$ positions. For example, the aristotype HgS has $x_{\text{Hg}} = 0.720$

TABLE IV. Summary of the two alternative descriptions of Buerger's rhombohedral intermediate ionic arrangement (Ref. 57) in terms of monoclinic (KOH-type) (Ref. 39), and trigonal (cinnabar-type) (Ref. 12) structures. Their structural relationship to the low pressure rocksalt and high-pressure CsCl structures is also given.

Model	Space group	Ionic positions	Rocksalt equivalence	CsCl equivalence
Trigonal (Cinnabar structure)	$P3_121$	$3(a)x,0,1/3: x=2/3$ $3(b)x,0,5/6: x=2/3$	$a_{\text{Cinna}} = a_{\text{RS}}/\sqrt{2}$ $c_{\text{Cinna}} = \sqrt{3}a_{\text{RS}}$	$a_{\text{Cinna}} = \sqrt{2}a_{\text{CsCl}}$ $c_{\text{Cinna}} = \sqrt{3}a_{\text{CsCl}}$
Monoclinic (KOH structure)	$P2_1$	$2(a)x,y,z: x=1/4, y=1/4, z=1/4$ $2(a)x,y,z: x=1/4, y=1/4, z=3/4$	$a_{\text{KOH}} = a_{\text{RS}}/\sqrt{2}$ $b_{\text{KOH}} = a_{\text{RS}}/\sqrt{2}$ $c_{\text{KOH}} = a_{\text{RS}}$ $\beta_{\text{KOH}} = 90^\circ$	$a_{\text{KOH}} = a_{\text{CsCl}}$ $b_{\text{KOH}} = \sqrt{2}a_{\text{CsCl}}$ $c_{\text{KOH}} = \sqrt{3}a_{\text{CsCl}}$ $\beta_{\text{KOH}} = \cos^{-1}(1/\sqrt{3}) = 125.27^\circ$

and $x_S = 0.485$ (Ref. 23). Nunes *et al.*¹² speculate that the poor agreement between the intensities in the original x-ray-diffraction study³⁷ and those calculated using typical values for x_{Ag} and x_{Cl} supports their idealized trigonal (cinnabar) model. However, attempts to refine the diffraction data collected in this work within the high-pressure phases AgCl-II, AgBr-II, and AgI-V using both the idealized and typical values for x_{Ag} and x_{anion} were not successful and do not support this model.

Model 2. An alternative lower symmetry description of the intermediate structure between the rocksalt and CsCl modifications has been provided by Kusaba *et al.*³⁹ In this model, Buerger's rhombohedral cell is considered as a monoclinic unit cell containing two formula units. In their chosen space group, $P2_1$, both ionic species are located in the general Wyckoff positions at x,y,z , with $x_A = y_A = z_A = 1/4$, $x_B = y_B = 1/4$ and $z_B = 3/4$. This arrangement can be considered to be an idealized version of the KOH structure and is identical to the idealized cinnabar structure discussed above. As shown in Table IV, the route from rocksalt to CsCl involves continuous changes in the unit-cell constants, the most significant being the increase in the interaxial angle β from 90° to 125.27° . The values of the six positional parameters remain constant throughout. This behavior is illustrated schematically in Fig. 10. The sixfold coordination within the rocksalt configuration [Fig. 10(a)] increases to a $6+2$ environment in the KOH-structured modification [the two longer bonds being shown as dashed lines in Fig. 10(b)] and then to the regular eightfold coordination in the CsCl-structured phase [Fig. 10(c)].

With the exception of the assignment of the correct space group (see below), the observation of a KOH-type phase at high pressure is supported by our experimental results for AgCl, AgBr, and AgI. However, the work of Kusaba *et al.*³⁹ on AgCl reports only the unit cell of the KOH phase at one pressure and no refinements of the experimental data were performed to confirm this assignment and extract values for the ionic position parameters. Though not explicitly stated, the latter is presumably a consequence of their use of the energy-dispersive technique with its inherent problems of data normalization. The continuous nature of the rocksalt→CsCl structural transition could not then be confirmed by their data. As discussed in Secs. IV A, IV B, and IV C, the data collected in this work within the high-pressure phases AgCl-II, AgBr-II, and AgI-V can be successfully fitted using the KOH-type structure in space group $P2_1/m$, with the two ionic species in $2(e) x,1/4,z$ positions. Reduc-

ing the symmetry to $P2_1$, as proposed by Kusaba *et al.*,³⁹ makes the structure noncentrosymmetric and the y positions of both the Ag^+ and the anion are no longer constrained to take the value $1/4$. Attempts to refine the data with space group $P2_1$ did not significantly improve the quality of the fit to the experimental data or result in values of y for either the cation or anion that were significantly different from 0.25. We conclude, therefore, that the correct space group is $P2_1/m$.

The $\text{Ag}^+ - \text{Ag}^+$ and anion-anion distances are identical in the rocksalt structure with a value equal to $a_{\text{RS}}/\sqrt{2}$. They are also the same in the CsCl structure (with a distance of a_{CsCl}) and, as illustrated in Fig. 10(b), are equal in the idealized KOH intermediate arrangement. However, Tables I–III indicate that the refined values of the four positional parameters

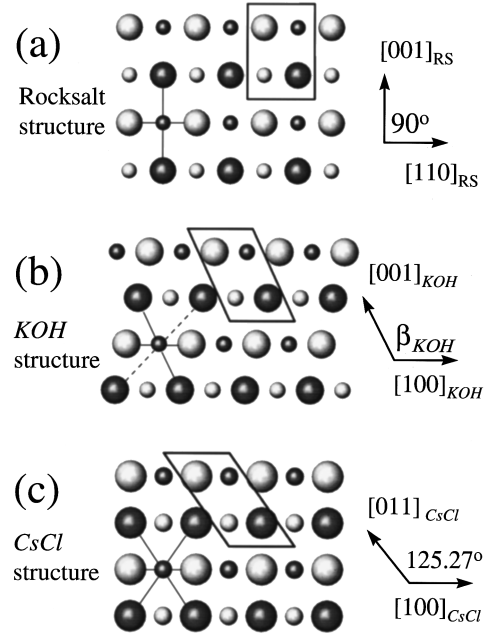


FIG. 10. Schematic diagram illustrating the continuous distortion of the rocksalt structure (a) to the CsCl structure (c) via the intermediate KOH arrangement (b) as the interaxial angle β increases from 90° to 125.27° . The small and large spheres represent the cations and anions, the dark spheres lying in the plane of the paper and the light ones being ions displaced by $\pm 1/2$ the repeat distance perpendicular to the plane of the paper. The coordination is illustrated in each case, the dashed lines denoting the two longer cation-anion contacts in the “ $6+2$ ” environment in the KOH structure (b).

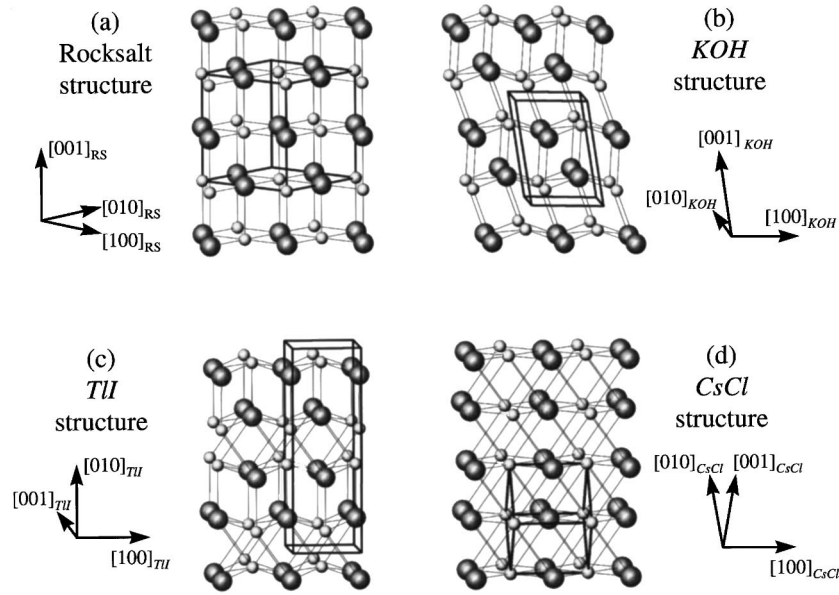


FIG. 11. The relationship between the ionic arrangements within the rocksalt (a), KOH (b), TII (c), and CsCl (d) structured polymorphs. The small and large spheres represent the cations and anions, respectively. The KOH and TII pictures use values of the unit-cell constants and positional parameters obtained for AgCl-II at $p = 8.6(1)$ GPa and AgCl-III at $p = 14.2(1)$ GPa. Both illustrate the tendency to form shorter $\text{Ag}^+ - \text{Ag}^+$ distances at the expense of longer $\text{Cl}^- - \text{Cl}^-$ ones. The crystallographic unit cells for each structure are illustrated by the dark lines.

x_{Ag} , z_{Ag} , x_{anion} , and z_{anion} are significantly different from their ideal values given in Table IV. The significance of these changes is illustrated in Fig. 11(b) for the case of KOH-structured AgCl-II at $p = 8.6(1)$ GPa. The distortions from the idealized structure allow the $\text{Ag}^+ - \text{Ag}^+$ distances to become slightly shorter than the $\text{Cl}^- - \text{Cl}^-$ ones, as might be expected owing to their different sizes [$r_{\text{Ag}^+} = 1.15$ Å and $r_{\text{Cl}^-} = 1.81$ Å (Ref. 58)]. This argument presumably explains the somewhat greater deviation from the ideal values shown in Table III by AgI [which has $r_{\text{I}^-} = 2.20$ Å (Ref. 58)], especially in the case of x_{Ag} . Tables I–III also indicate that the positional parameters generally move further away from their ideal values as pressure increases. This feature will be considered later in this section.

We now turn our attention to the TII structure adopted by phase AgCl-III. This structure is illustrated in Fig. 11(c). Both species are located in 4(c) sites of space group $Cmcm$ at $0, y, 1/4$ with $y_{\text{Ag}} \sim 0.40$ and $y_{\text{Cl}} \sim 0.14$ (Table I). With reference to Fig. 11(c), it is clear that the TII arrangement is related to the KOH structure and that both are derivatives of the rocksalt structure [Fig. 11(a)]. Kusaba *et al.*³⁹ proposed that the orthorhombic unit cell of the TII-structured phase AgCl-II (of dimensions $a_{\text{TII}} \times b_{\text{TII}} \times c_{\text{TII}}$) could be interpreted in terms of an effective monoclinic cell corresponding to that in the KOH structure (with unit-cell constants a'_{KOH} , b'_{KOH} , c'_{KOH} , and β'_{KOH}). The relevant expressions are

$$a'_{\text{KOH}} = a_{\text{TII}},$$

$$b'_{\text{KOH}} = c_{\text{TII}},$$

$$c'_{\text{KOH}} = b_{\text{TII}}/2 \sin \beta'_{\text{KOH}}$$

and

$$\beta'_{\text{KOH}} = 90 + \tan^{-1}(a_{\text{TII}}/b_{\text{TII}}).$$

In the case of our data for AgCl-II at $p = 14.2(1)$ GPa, we obtain values $a'_{\text{KOH}} = 3.337(1)$ Å, $b'_{\text{KOH}} = 4.095(1)$ Å, $c'_{\text{KOH}} = 5.227(1)$ Å, and $\beta'_{\text{KOH}} = 108.6(1)^\circ$. As discussed by Kusaba *et al.*,³⁹ these values follow the general trend expected for the continuous monoclinic transition from the rocksalt structure to the CsCl one, in particular with respect to the increasing value of the monoclinic interaxial angle from 90° to 125.27° . However, this approach is rather misleading, since the ionic arrangement within the TII structure is different from the KOH arrangement. In particular, they cannot be derived from one another using only the degrees of freedom allowed by their respective space-group symmetries. In the case of the rocksalt \rightarrow KOH \rightarrow CsCl continuous transformation [Fig. 11(a) \rightarrow Fig. 11(b) \rightarrow Fig. 11(d)], the gradual increase in the value of β causes the relative displacement of all the $(001)_{\text{KOH}}$ planes in the $[100]_{\text{KOH}}$ direction. However, the TII arrangement is unlike the KOH (and cinnabar) intermediate structures because it cannot be directly deformed to produce both the low-pressure rocksalt and high-pressure CsCl configurations. Instead, the rocksalt \rightarrow TII \rightarrow CsCl route [Fig. 11(a) \rightarrow Fig. 11(c) \rightarrow Fig. 11(d)] is a two-stage discontinuous process, requiring the displacement of pairs of $(010)_{\text{TII}}$ planes in the $[100]_{\text{TII}}$ direction. With reference to Fig. 11, the rocksalt \rightarrow TII transformation requires the movement of the second and third layers from the bottom of the picture by $a_{\text{TII}}/2$ and the subsequent TII \rightarrow CsCl one uses a similar shift of the third and fourth layers. This idealized picture assumes that the $(010)_{\text{TII}}$ planes in AgCl-III are flat, which would be true if $y_{\text{Ag}} = 3/8$ and $y_{\text{Cl}} = 1/8$. In reality, the environment around both Ag^+ and Cl^- is a distorted sevenfold coordination, as illustrated in Fig. 11(c). In common with the situation in KOH-structured AgCl-II, the refined values of the positional parameters

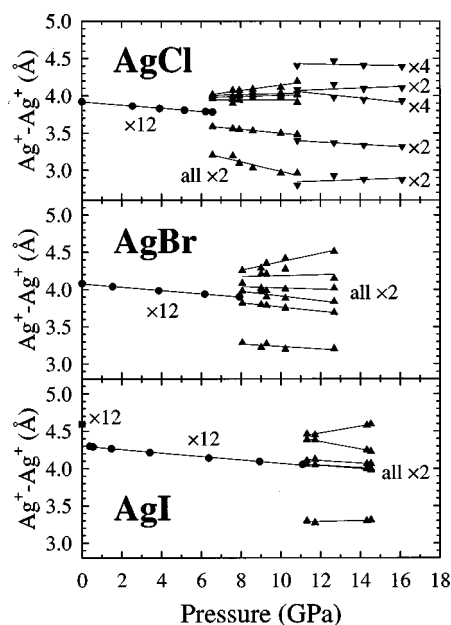


FIG. 12. The pressure variation of the $\text{Ag}^+\text{-Ag}^+$ distances in AgCl, AgBr, and AgI. The symbols represent different structure types: \blacksquare zincblende (AgI-II'); \bullet rocksalt (AgCl-I, AgBr-I, AgI-III); \blacktriangle KOH (AgCl-II, AgBr-II, AgI-V); \blacktriangledown TII (AgCl-III). The two lowest pressure data points in the rocksalt-structured phase AgI-III are taken from Ref. 45.

(Table I) are somewhat displaced from their ideal values and the structure favors shorter $\text{Ag}^+\text{-Ag}^+$ distances and longer $\text{Cl}^-\text{-Cl}^-$ ones. For this reason, we might then expect the TII arrangement to be favored in binary AB compounds possessing ions of different size. Indeed, very recent x-ray-diffraction studies of NaBr and NaI indicate that these alkali

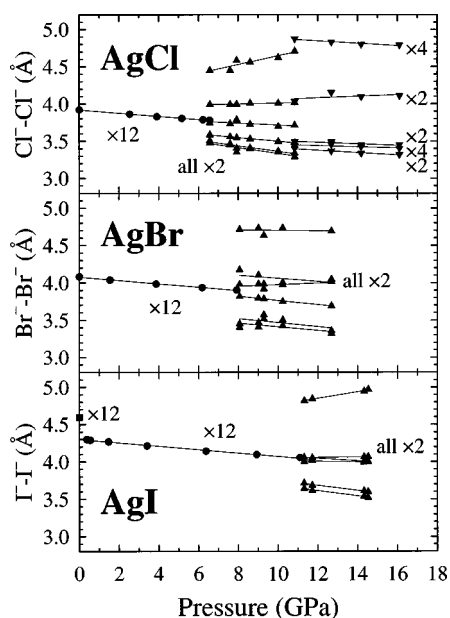


FIG. 13. The pressure variation of the anion-anion distances in AgCl, AgBr, and AgI. The symbols represent different structure types: \blacksquare zincblende (AgI-II'); \bullet rocksalt (AgCl-I, AgBr-I, AgI-III); \blacktriangle KOH (AgCl-II, AgBr-II, AgI-V); \blacktriangledown TII (AgCl-III). The two lowest pressure data points in the rocksalt-structured phase AgI-III are taken from Ref. 45.

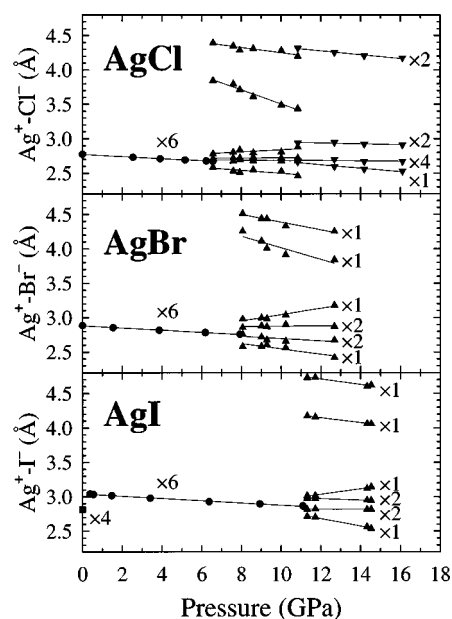


FIG. 14. The pressure variation of the $\text{Ag}^+\text{-anion}$ distances in AgCl, AgBr, and AgI. The symbols represent different structure types: \blacksquare zincblende (AgI-II'); \bullet rocksalt (AgCl-I, AgBr-I, AgI-III); \blacktriangle KOH (AgCl-II, AgBr-II, AgI-V); \blacktriangledown TII (AgCl-III). For clarity, the multiplicities of the bond lengths in the KOH structured phase AgCl-II are not shown, but are the same as those given for the isostructural phases AgBr-II and AgI-V in the lower plots. The two lowest pressure data points in the rocksalt-structured phase AgI-III are taken from Ref. 45.

halide compounds adopt TII-structured phases at $p \sim 30\text{--}40$ GPa (Ref. 59). The Li^+ halides, with even greater cation-anion size difference might also be expected to adopt this structure at higher pressures.

Figures 12–14 show the pressure variation of the various interionic distances within the three Ag(I) halides. In the rocksalt arrangement, the cation and anion sublattices form two cubic close-packed (c.c.p.) arrays displaced by a distance $\sqrt{3}a_{\text{RS}}/2$ along the body diagonal. The data for the $\text{Ag}^+\text{-Ag}^+$ and anion-anion distances (Figs. 12 and 13, respectively) are broadly similar though, as discussed already, the former are somewhat shorter in the KOH and TII-structured polymorphs to reflect the smaller size of the cations. There is an increasing distortion of the two pseudo-c.c.p. sublattices within the three KOH-structured phases and relatively little change within the TII-structured AgCl-III. The behavior of the $\text{Ag}^+\text{-anion}$ distances on increasing pressure is more marked (Fig. 14), though relatively similar for all three isostructural KOH-type phases. At the rocksalt \rightarrow KOH structural transition the perfect octahedral coordination surrounding the cation becomes distorted with four different $\text{Ag}^+\text{-anion}$ distances which differ by only $\sim 6\text{--}8\%$. However, the most significant change is the appearance of two further contacts at distances of $\sim 4\text{--}4.5$ Å. These correspond to the bonds illustrated as dashed lines in Fig. 10(b). The effect of the “nonideal” values of the unit-cell constants and positional parameters is to make these two longer contacts in the “6+2” coordination shell different. However, both become closer to the other six as pressure increases, principally due to the increase in the β angle and the decrease in x_{Ag} . In the TII-structured phase AgCl-III, the

six closer Ag^+-Cl^- distances are replaced by seven of comparable length in the range 2.5–3.0 Å, with the next-nearest anions significantly further away (~4.3 Å).

VI. CONCLUSIONS

The high-pressure structural behavior of AgCl, AgBr, and AgI has been determined by high-pressure angle-dispersive x-ray diffraction measurements to $p \sim 13$ –16 GPa. Though the pressure range is too limited to observe the complete transformation sequence, the transition from the sixfold coordinated rocksalt structure to the eightfold-coordinated CsCl arrangement appears to be similar in all three compounds. This occurs via two rocksalt-related intermediate phases, with the monoclinic KOH and orthorhombic TII structures. If we consider only the unit-cell dimensions, the trends in the structural behavior appear broadly consistent with the continuous displacive rhombohedral model proposed by Buerger⁵⁷ and subsequently predicted by *ab initio* electronic structure calculations¹² and used to interpret energy-dispersive x-ray diffraction studies.³⁹ However, the accurate characterization of the ionic positions in this work show that the structural evolution under pressure is considerably more complex than predicted by such idealized models, principally as a means of accommodating shorter Ag^+-Ag^+ distances at the expense of longer distances between nearest-neighbor halide anions.

It is interesting to note, however, that the structural sequence rocksalt→KOH→TII→CsCl is not particularly unusual. The various MOH and MOD compounds (where $M = \text{K}, \text{Na}, \text{Rb}, \text{and Cs}$) adopt rocksaltlike phases at elevated temperatures with freely rotating OH^- and, on decreasing temperature and/or increasing pressure, the OH^- motion becomes hindered and the compounds adopt KOH and TII-type configurations.^{60–65} It would be interesting to know whether these MOH and MOD compounds undergo a TII→CsCl transition at higher pressures, of the type observed in TII itself at $p = 0.5$ GPa (Ref. 66). In these systems it is generally

believed that the preference for the KOH and TII-type structures is a means of achieving a more efficient packing arrangement with nonspherical ions, the deformation of the electron cloud being caused by the OH^- in KOH and the $6s^2$ electron lone pair of Tl^+ in TII. Presumably, the adoption of these structures in AgCl, AgBr, and AgI is a manifestation of the significant covalent character, with the direct transition between the high-symmetry cubic rocksalt and CsCl structures favored in predominantly ionic compounds which possess isotropic bonds, such as the alkali halides.

Finally, in assessing the success of the theoretical models to predict *ab initio* the high-pressure behavior of such systems it is clearly necessary to discount those papers which assume that the first pressure-induced transition is to the CsCl-type structure.⁶⁷ The findings presented in this work do not support the recent theoretical findings of Nunes *et al.*,¹² which favor a continuous transformation in AgCl and AgBr via a cinnabarlike phase. In the case of AgI, the prediction of an unspecified intermediate phase is borne out in this work and it would be interesting to see the results of testing the KOH- and TII-type structures with this method. Clearly, the lower symmetry and greater number of degrees of freedom (unit-cell constants and positional parameters) would make such calculations time consuming. Nevertheless, it is hoped that the high-quality structural information presented in this paper will motivate further theoretical studies of the effects of hydrostatic pressure on compounds of this type.

ACKNOWLEDGMENTS

We are extremely grateful to R. J. Nelmes, M. I. McMahon, N. G. Wright, and D. R. Allan for their assistance during the experiment and for the use of their equipment and data reduction software. The work presented in this paper forms part of a wider research project investigating the high-pressure behavior of binary copper and silver compounds funded by the United Kingdom Engineering and Physical Sciences Research Council (Reference No. P:AK:113 C2).

*Corresponding author. FAX: +44 01235 445720; electronic address: sh@isise.rl.ac.uk

¹J. M. Besson, R. J. Nelmes, G. Hamel, J. S. Loveday, G. Weill, and S. Hull, *Physica B* **180&181**, 907 (1992).

²R. J. Nelmes and M. I. McMahon, *J. Synchrotron Radiat.* **1**, 69 (1994).

³J. R. Chelikowsky and J. K. Burdett, *Phys. Rev. Lett.* **56**, 961 (1986).

⁴J. R. Chelikowsky, *Phys. Rev. B* **35**, 1174 (1987).

⁵N. E. Christensen, S. Satpathy, and Z. Pawlowska, *Phys. Rev. B* **36**, 1032 (1987).

⁶J. Crain, R. O. Piltz, G. J. Ackland, S. J. Clark, M. C. Payne, V. Milman, J. S. Lin, P. D. Hatton, and Y. H. Nam, *Phys. Rev. B* **50**, 8389 (1994).

⁷H. C. Hsueh, J. R. MacLean, G. Y. Guo, M. H. Lee, S. J. Clark, G. J. Ackland, and J. Crain, *Phys. Rev. B* **51**, 12 216 (1995).

⁸S. Froyen and M. L. Cohen, *Phys. Rev. B* **28**, 3258 (1983).

⁹F. Kirchhoff, J. M. Holender, and M. J. Gillan, *Phys. Rev. B* **49**, 17 420 (1994).

¹⁰R. H. Victoria, *Phys. Rev. B* **56**, 4417 (1997).

¹¹G. S. Nunes, P. B. Allen, and J. L. Martins, *Solid State Commun.* **105**, 377 (1998).

¹²G. S. Nunes, P. B. Allen, and J. L. Martins, *Phys. Rev. B* **57**, 5098 (1998).

¹³R. E. Hanneman, M. D. Banus, and H. C. Gatos, *J. Phys. Chem. Solids* **25**, 293 (1964).

¹⁴S. C. Yu, I. L. Spain, and E. F. Skelton, *Solid State Commun.* **25**, 49 (1978).

¹⁵C. S. Menoni and I. L. Spain, *Phys. Rev. B* **35**, 7520 (1987).

¹⁶J. Z. Hu, *Solid State Commun.* **63**, 471 (1987).

¹⁷R. J. Nelmes, M. I. McMahon, and S. A. Belmonte, *Phys. Rev. Lett.* **79**, 3668 (1997).

¹⁸For a discussion of the high-pressure structural behavior of the III-V and II-VI semiconductors, including the (non)existence of site-(ordered)/disordered β -Sn-structured phases, see R. J. Nelmes and M. I. McMahon, *Semicond. Semimet.* **54**, 145 (1998).

¹⁹Y. E. Tonkov, *High Pressure Phase Transformations. A Handbook* (Gordon and Breach, London, 1992).

²⁰R. J. Hemley, *Science* **281**, 1296 (1998).

²¹M. I. Eremets, K. Shimizu, T. C. Kobayashi, and K. Amaya, *Science* **281**, 1333 (1998).

²²J. C. Phillips, *Rev. Mod. Phys.* **42**, 317 (1970).

- ²³R. W. G. Wyckoff, *Crystal Structures* (Interscience, New York, 1963), Vol. 1.
- ²⁴G. Burley, *Acta Crystallogr.* **23**, 1 (1967).
- ²⁵J. F. Hamilton, *Adv. Phys.* **37**, 359 (1988).
- ²⁶S. Hull and D. A. Keen, *Europhys. Lett.* **23**, 129 (1993).
- ²⁷S. Hull and D. A. Keen, *Phys. Rev. B* **50**, 5868 (1994).
- ²⁸M. Hofmann, S. Hull, and D. A. Keen, *Phys. Rev. B* **51**, 12 022 (1995).
- ²⁹S. Hull and D. A. Keen, *J. Phys.: Condens. Matter* **8**, 6191 (1996).
- ³⁰P. M. Halleck, J. C. Jamieson, and C. W. F. T. Pistorius, *J. Phys. Chem. Solids* **33**, 769 (1972).
- ³¹S. Hull and P. Berastegui, *J. Phys.: Condens. Matter* **10**, 7945 (1998).
- ³²P. W. Bridgman, *Proc. Am. Acad. Arts Sci.* **76**, 1 (1945).
- ³³T. E. Slykhouse and H. G. Drickamer, *J. Phys. Chem. Solids* **7**, 207 (1958).
- ³⁴W. A. Bassett and T. Takahashi, *Am. Mineral.* **50**, 1576 (1965).
- ³⁵B. M. Riggelman and H. G. Drickamer, *J. Chem. Phys.* **38**, 2721 (1963).
- ³⁶J. C. Jamieson and A. W. Lawson, *J. Appl. Phys.* **33**, 776 (1962).
- ³⁷R. N. Schock and J. C. Jamieson, *J. Phys. Chem. Solids* **30**, 1527 (1969).
- ³⁸S. S. Kabalkina, M. O. Shcherbakov, and L. F. Vereshchagin, *Sov. Phys. Dokl.* **15**, 751 (1971).
- ³⁹K. Kusaba, Y. Syono, T. Kikegawa, and O. Shimomura, *J. Phys. Chem. Solids* **56**, 751 (1995).
- ⁴⁰L. Merrill and W. A. Bassett, *Rev. Sci. Instrum.* **45**, 290 (1974).
- ⁴¹R. O. Piltz, M. I. McMahon, J. Crain, P. D. Hatton, R. J. Nelmes, R. J. Cernik, and G. Bushnell-Wye, *Rev. Sci. Instrum.* **63**, 700 (1992).
- ⁴²J. Rodriguez-Carvajal (unpublished).
- ⁴³B. E. Mellander, J. E. Bowling, and B. Baranowski, *Phys. Scr.* **22**, 541 (1980).
- ⁴⁴B. E. Mellander, *Phys. Rev. B* **26**, 5886 (1982).
- ⁴⁵D. A. Keen and S. Hull, *J. Phys.: Condens. Matter* **5**, 23 (1993).
- ⁴⁶J. L. Tallon, *Phys. Rev. B* **38**, 9069 (1988).
- ⁴⁷D. A. Keen, S. Hull, W. Hayes, and N. J. G. Gardner, *Phys. Rev. Lett.* **77**, 4914 (1996).
- ⁴⁸A. March, *Z. Kristallogr.* **81**, 285 (1932).
- ⁴⁹F. Birch, *J. Geophys. Res.* **57**, 227 (1952).
- ⁵⁰K. F. Loje and D. E. Schuele, *J. Phys. Chem. Solids* **31**, 2051 (1970).
- ⁵¹D. S. Tannhauser, L. T. Bruner, and A. W. Lawson, *Phys. Rev.* **102**, 1276 (1956).
- ⁵²W. Hidshaw, J. T. Lewis, and C. V. Briscoe, *Phys. Rev.* **163**, 876 (1967).
- ⁵³T. Yagi, T. Suzuki, and S-I. Akimoto, *J. Phys. Chem. Solids* **44**, 135 (1983).
- ⁵⁴H. H. Demarest, C. R. Cassell, and J. C. Jamieson, *J. Phys. Chem. Solids* **39**, 1211 (1978).
- ⁵⁵T. Chattopadhyay, A. Werner, H. G. von Schnering, and J. Panetier, *Rev. Phys. Appl.* **19**, 807 (1984).
- ⁵⁶A. Onodera, Y. Nakai, S. Kawano, and N. Achiwa, *High Temp.-High Press.* **24**, 55 (1992).
- ⁵⁷M. J. Buerger, *Fortschr. Mineral.* **39**, 9 (1961).
- ⁵⁸R. D. Shannon and C. T. Prewitt, *Acta Crystallogr., Sect. B: Struct. Crystallogr. Cryst. Chem.* **25**, 925 (1969).
- ⁵⁹J. M. Léger, J. Haines, C. Danneels, and L. S. de Oliveira, *J. Phys.: Condens. Matter* **10**, 4201 (1998).
- ⁶⁰H. Jacobs, J. Kockelkorn, and T. Tacke, *Z. Anorg. Allg. Chem.* **531**, 119 (1985).
- ⁶¹B. Mach, H. Jacobs, and W. Schäfer, *Z. Anorg. Allg. Chem.* **553**, 187 (1987).
- ⁶²H. Jacobs, B. Mach, H. D. Lutz, and J. Henning, *Z. Anorg. Allg. Chem.* **544**, 28 (1987).
- ⁶³H. Jacobs, B. Mach, B. Harbrecht, H. D. Lutz, and J. Henning, *Z. Anorg. Allg. Chem.* **544**, 55 (1987).
- ⁶⁴J. W. Otto and W. B. Holzappel, *J. Phys.: Condens. Matter* **7**, 5461 (1995).
- ⁶⁵J. S. Loveday, W. G. Marshall, R. J. Nelmes, S. Klotz, G. Hamel, and J. M. Besson, *J. Phys.: Condens. Matter* **8**, L597 (1996).
- ⁶⁶G. A. Samara, L. C. Walters, and D. A. Northrop, *J. Phys. Chem. Solids* **11**, 92 (1967).
- ⁶⁷D. C. Gupta and R. K. Singh, *Phys. Rev. B* **43**, 11 185 (1991).